Eur Biophys J (2007) 36:609–620
DOI 10.1007/s00249-007-0130-x

ORIGINAL PAPER

Liposome complexation efficiency monitored by FRET: effect of charge ratio, helper lipid and plasmid size

Catarina Madeira · Luís M. S. Loura · Manuel Prieto · Aleksander Fedorov · M. Raquel Aires-Barros

Received: 21 March 2006 / Revised: 21 December 2006 / Accepted: 2 January 2007 / Published online: 30 January 2007

Abstract Cationic lipid/DNA complexes (lipoplexes) are promising vehicles for DNA vaccines or gene therapy. In these systems, transfection efficiency is highly related to lipoplex charge ratio, since lipoplexes with charge ratios (±) lower than electroneutrality have most DNA uncovered by the liposomes, and thus are unprotected from enzyme degradation. However, a large excess of cationic lipids is undesirable because of eventual cytotoxicity. The aim of this work was to determine the minimum charge ratio from which all DNA molecules are complexed by the liposomes varying the lipid formulation and plasmid size, using a new FRET (fluorescence resonance energy transfer) methodology. The similarity of FRET results, fluorescence intensity data and fluorescence decays of several charge ratios above (±) ≥ 4 or 5 confirmed that once all DNA is covered by the liposomes, additional lipid molecules do not affect the lipoplex multilamellar repeat distance. It was also verified by FRET that the presence of helper lipid reduces the amount of cationic lipid required for DNA protection but does not affect the lipoplex multilamellar repeat distance. This distance varies with the plasmid size when supercoiled plasmid is used, being apparently larger when longer plasmids are used. Our study indicates that, despite the complexity of these systems not being totally described by our model, FRET is an informative technique in lipoplex characterization.

Keywords FRET · Lipoplex · BOBO-1 · Cationic lipid · Plasmid DNA · Gene delivery

Abbreviations

BOBO-1	Benzothiazolium, 2,2′-[1,3-propanediylbis[(dimethyliminio)-3,1-propanediyl-1(4H)-pyridinyl-4-ylidenemethylidyne]]bis[3-methyl]-, tetraiodide
DOTAP	1,2-dioleoyl-3-trimethylammonium-propane
YOYO-1	1,1′-[1,3- propanediylbis[(dimethyliminio)-3,1- propanediyl]]bis[4-[(3-methyl-2(3H)-benzoxazolylidene)methyl]]-, tetraiodide

C. Madeira · M. R. Aires-Barros (✉)
Centro de Engenharia Biológica e Química,
Instituto Superior Técnico,
Av. Rovisco Pais 1049-001, Portugal
e-mail: pcbarros@alfa.ist.utl.pt

L. M. S. Loura
IBB-Institute for Biotechnology and Bioengineering,
Centre for Biological and Chemical Engineering,
Universidade de Évora, Rua Romão Ramalho,
7000-671 Évora, Portugal

M. Prieto · A. Fedorov
Centro de Química-Física Molecular,
Complexo I, Instituto Superior Técnico,
Av. Rovisco Pais 1049-001, Portugal

Introduction

Among the non-viral vectors, cationic liposomes seem to be the most widely used DNA delivery system (Huang et al. 1999). Despite low transfection efficiencies, they show non-immunogenicity, low toxicity and possibility of large-scale production. Many efforts have

been made to fully characterize cationic liposome–DNA complexes (lipoplexes), because it is the only way to understand, improve and control the transfection efficiency of these non-viral based vectors. Since 1987, most of the published data regard the optimization of lipid formulations and measurement of the transfection efficiency as a function of DNA/lipid charge ratio (Farhood et al. 1995; Hong et al. 1997; Lee and Huang 1996; Ross and Hui 1999; Simões et al. 2000; Smisterová et al. 2001; Templeton et al. 1997; Thierry et al. 1997; Zhou and Huang 1994). In parallel with several lipoplex physical-chemistry studies (Ferrari et al. 2001; Gershon et al. 1993; Perrie and Gregoriadis 2000; Zuidam et al. 1999b) other techniques were used to visualize lipoplex structure (Kreiss et al. 1999; Oberle et al. 2000; Rädler et al. 1997). Electron microscopy and X-ray diffraction used in parallel revealed a multilamellar structure of lipid bilayers with sandwiched DNA, with a constant interlayer spacing invariant with the charge ratio, and depending on cationic liposomes formulations (Lasic et al. 1997; Rädler et al. 1997).

In recent years, the use of the fluorescence resonance energy transfer (FRET) methodology has allowed further insights into the lipoplex structure and behaviour in solution. FRET using one dye on the DNA and other on the lipid has been recently used in lipoplex characterization, albeit in a qualitative way. This methodology is suitable for the study of DNA–lipid interactions (Clamme et al. 2000; Zhang et al. 2003), to evaluate DNA condensation by surfactants (Itaka et al. 2002; Lleres et al. 2001), or to monitor the interaction of the formed complexes with membrane model systems (Lleres et al. 2002). An assay relying on FRET also allowed to distinguish between DNA attached to the cell surface and internalized (Wong et al. 2001). The use of FRET to estimate the distance of closest approach of DNA to the lipid bilayers was recently reported (Wiethoff et al. 2002).

Previously, using a unique lipoplex formulation (DOTAP/pUC19), we proposed the use of a new FRET methodology to calculate the lipoplex multilamellar distance and liposome complexation efficiency (Madeira et al. 2003) taking advantage of the knowledge that those lipoplexes have a lamellar structure, and that multilamellar distances do not vary with the lipoplex charge ratios (Caracciolo et al. 2002; Kreiss et al. 1999; Radler et al. 1998). In this work, using different liposomal formulations (including zwitterionic helper lipid) and plasmid DNA sizes, the same FRET methodology is used to evaluate and compare the multilamellar distances and complexation efficiencies.

Materials and methods

Materials

The plasmid pVAX1LacZ with 6,050 bp was purchased from Invitrogen (Carlsbad, CA). Plasmid pVAX1lacZp25 with 6,717 bp was constructed in the laboratory of the Center of Biological and Chemical Engineering, by cloning a gene that encodes for an envelope protein of the virus *Maedi-Visna* (p25) in the plasmid pVAX1LacZ. For the sake of simplicity, the plasmids pVAX1LacZ and pVAX1LacZp25 will be referred to as pVAX and pVAX25, respectively. The cationic and neutral lipids, 1,2-dioleoyl-3-trimethylammonium-propane (DOTAP) and 1,2-dioleoyl-*sn*-glycero-3-phosphoethanolamine (DOPE), respectively, were obtained from Avanti Polar Lipids (Alabaster, AL). The membrane dye 2-(4,4-difluoro-5-octyl-4-bora-3a,4a-diaza-s-indacene-3-pentanoyl)-1-hexadecanoyl-*sn*-glycero-3-phosphocoline (BODIPY-PC) as well as the DNA intercalating dyes benzothiazolium, 2,2′-[1,3-propanediylbis[(dimethyliminio)-3,1-propanediyl-1(4H)-pyridinyl-4-ylidenemethy-lidyne]] bis[3-methyl]-tetraiodid (BOBO-1) and ethidium bromide (EtBr), were obtained from Molecular Probes (Eugene, OR). Lipids and dyes' structures are shown in Fig. 1. Liposomes and lipoplexes were prepared in 30 mM Tris (hydroxymethyl)-aminomethan buffer, pH 7.4 adjusted with hydrochloric acid (Tris–HCl). Electrophoresis was performed with agarose obtained from FCM (Rockland, ME). TAE (0.04 M Tris-acetate, 0.001 M EDTA) was the buffer used to run the electrophoresis gel, for which Tris base, glacial acetic acid and EDTA were purchased from Sigma (Saint Louis, MO). LB Broth, used to culture *Escherichia coli*, for plasmid production was also obtained from Sigma (Saint Louis, MO).

DNA purification and quantification

The plasmids were replicated in *E. coli* (DH5α) and purified employing a Qiagen Plasmid Midi Kit procedure (Valencia, CA). DNA concentration was measured spectrophotometrically (50 μg/mL of double stranded DNA has an absorbance of 1 at 260 nm). Its purity and integrity was assessed using agarose gel electrophoresis. All plasmid preparations showed a major amount of super coiled plasmid and a minor amount of relaxed plasmid. Working solutions of BOBO-1 were prepared immediately prior to use by diluting the dimethylsulphoxide stock solution with the working buffer. The dye/DNA solutions were always prepared by adding an adequate amount of DNA to a

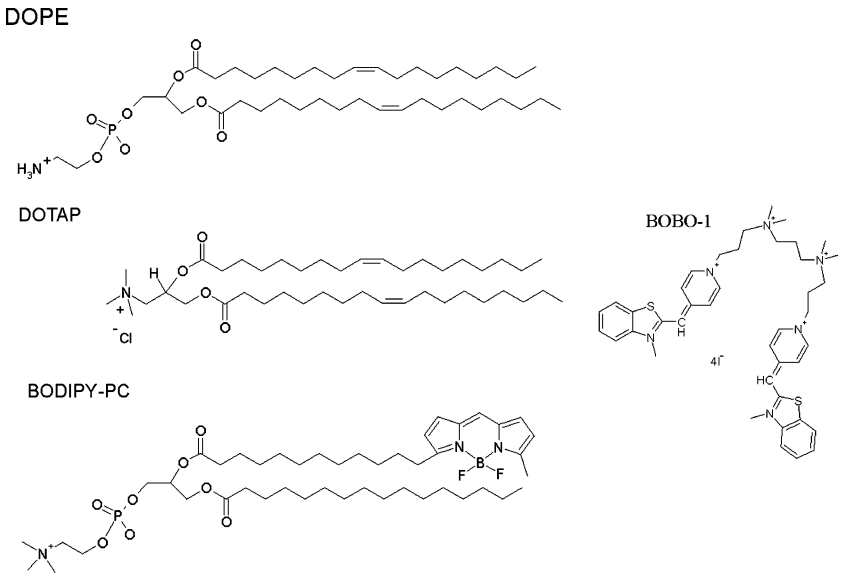

Fig. 1 Chemical structures of neutral and cationic lipid, *DOPE* and *DOTAP*, respectively, and the fluorescently labelled lipid *BODIPY-PC* and the cyanine dye (*BOBO-1*) used in this work

larger volume of dye in the working solution, to yield the desired dye: DNA ratio (dye molecule/DNA base). The dye/DNA complex was allowed to equilibrate for at least 30 min, at 20°C, before adding DOTAP or carrying out any measurement. All solutions containing membrane or intercalator dyes were protected from light between preparation and measurements.

Liposome and lipoplex preparation

Cationic liposomes were prepared as described elsewhere (Madeira et al. 2003). Fluorescently labelled liposomes were obtained by adding the adequate amount of probe to the chloroform solution. The exact probe concentration is indicated where appropriate. The lipoplexes (cationic liposomes–DNA complexes) were obtained by direct and rapid addition of an appropriate amount of the cationic lipid dispersion to the DNA plasmid solution at various charge ratios (DOTAP/DNA between 0.001 and 18), by rapidly adding equal volumes, with equal final DNA concentration in all samples. The complexes were incubated at room temperature for 30 min, minimum, before use.

Agarose gel electrophoresis

Characterization of all plasmid batches and dye/plasmid complexes was carried out by loading samples (20 μL) in a 0.8 % agarose gel, under a constant electric field of 2.0 V/cm with 40 mM Tris-acetate, 1 mM EDTA (TAE) as electrophoresis buffer. Lipoplexes samples, 40 μL, were also analysed by electrophoresis using the same procedure. All the gels were post-stained in EtBr (0.5 μg/mL) for 30 min and then visualized, integrated and photographed with an ultraviolet transillumination equipment (Eagle Eye II, vers.1.1, Stratagene (Cedar Creek, TX)) with a CCD camera system.

Steady-state fluorescence measurements

Fluorescence spectra and steady-state measurements were carried out with a SLM-Aminco 8100 Series 2 spectrofluorimeter (Rochester, NY; with double excitation and emission monochromators, MC-400) in a right-angle geometry. The light source was a 450-W Xe arc lamp and the reference was a Rhodamine B quantum counter solution. Correction of excitation and emission spectra was performed using the apparatus correction software. 5 × 5-mm quartz cuvettes were used. Fluorescence intensities were measured at λ_{exc} = 465 nm and λ_{em} = 490 nm for BOBO-1, with spectral bandwidths of 4 nm.

Emission spectra were recorded at the following excitation wavelengths: λ_{exc} (BODIPY) = 465 nm; λ_{exc} (BOBO) = 430 nm. For excitation spectra measurements, emission wavelengths λ_{em} (BODIPY) = 610 nm; λ_{em} and (BOBO) = 520 nm were used. The fluorescence quantum yields of BOBO-1 in the presence of DNA (Φ_B) and within lipoplexes (Φ_{BL}) were determined as described elsewhere (Madeira et al. 2003).

Fluorescence decay measurements

Fluorescence decay measurements were carried out with a single photon-timing system. For excitation of

BOBO-1 at 287 nm, a frequency doubled, cavity dumped, dye laser of Rhodamine (Rh) 6G (Coherent 701-2), synchronously pumped by a mode-locked Ar^+ laser (514.5 nm, Coherent Innova 400-10) was used (Coherent, Santa Clara, CA). Filters were added to a Jobin-Yvon (Edison, NJ) HR320 monochromator to further screen scattered excitation light, and isolate donor fluorescence from that of acceptor, respectively. For the detection, a Hamamatsu R-2809 MCP photomultiplier was used, and the instrumental response functions (50 ps full-width at half-maximum) for deconvolution were generated from scattering dispersion (Silica, colloidal water suspension, Aldrich, Milwaukee, WI). Emission [at 485 nm (Rh) and 435 nm (Ti-Sph)] was detected at the magic angle relative to the vertically polarized excitation beam. The number of counts on the peak channel was ≈20,000, and the number of channels per curve used for analysis was ≈ 1,000. Data analysis was carried out using non-linear, least squares iterative convolution method based on the Marquardt algorithm (Marquardt 1963). The goodness of the fits was judged from the Chi-square values (χ^2) and the lifetime-weighted quantum yields, $<\tau>$, were calculated according to

$$<\tau> = \sum_{i=1}^{n} \alpha_i \times \tau_i \tag{1}$$

where α_i and τ_i are the normalized pre-exponential factor (amplitude) and the lifetime, respectively, in n exponential decay components.

FRET assays

In FRET assays, lipoplexes were prepared with fluorescent dyes incorporated both in the DNA and in the liposomes. The dimeric cyanine dye, BOBO-1, was used as the donor and a *d/b* ratio (dye molecules/base number) of 0.01 was used, allowing 1 h 30 min of incubation. The membrane dye BODIPY-PC was the acceptor. Separately, several batches of liposomes were prepared with different dye concentrations with BODIPY-PC/DOTAP molar ratios ranging from 1:500 to 1:50. All the samples were protected from light since preparation until the end of measurements. The Förster distance was determined as described elsewhere (Madeira et al. 2003). For each charge ratio the donor average lifetime values (Eq. 1) in the absence of acceptor, and the fluorescence intensity of the donor in the presence of different acceptor concentrations were measured and used in the FRET model (Eq. 2).

FRET methodology

The equation for the decay of the donor in the presence of a plane of acceptors (Fig. 2), which assumes low density of excited acceptors, no energy migration among donors, no translational diffusion of probes during the donor excited state lifetime, uniform distribution of acceptors, a single Förster distance R_0 value for all donor-acceptor pairs, and probe dimensions << R_0 is given by (Madeira et al. 2003):

$$i_{DA}(t) = (1-\gamma) i_D(t) \exp\left(-\frac{2C}{\Gamma(2/3) b} \int_0^1 \frac{1-\exp(-t b^3 \alpha^6)}{\alpha^3} d\alpha \right) + \gamma i_{D0}(t) \tag{2}$$

where

$$C = \Gamma(2/3).n.\pi.R_0^2 \tau^{-1/3} \tag{3}$$

and

$$b = (R_0/d)^2 \tau^{-1/3} \tag{4}$$

In these equations, $i_D(t) = \exp(-t/\tau_D)$ is the donor decay in the absence of acceptor. For donors with non-exponential decay (as often is the case), $i_D(t)$ should be the experimental decay law (sum of exponentials) and τ in Eqs. 3 and 4 should be replaced by the average lifetime of the donor [e.g. (Loura et al. 2001)]. Γ is the complete gamma function, d is the interchromophore distance (Å), and n is the acceptor surface density [n = 2×(dye:lipid mole ratio)/(area per lipid molecule)]. For the used lipid probe, the difference in transverse location for chromophores belonging to labelled lipid molecules in opposing leaflets of the same bilayer is small for FRET purposes (<<R_0) and will

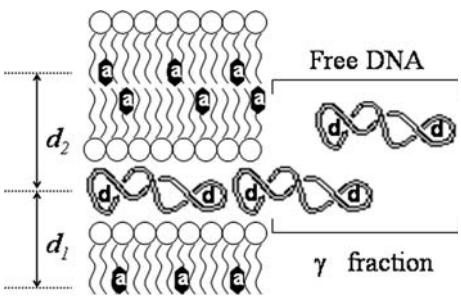

Fig. 2 Schematic representation of the lipoplexes multilamellar structure with the fluorescent probes within DNA and lipid. Acceptor (*a*) on the lipid (BODIPY-PC) and donor (*d*) on the DNA (BOBO-1)

from this point on be neglected (that is, we can take $d \approx d_1 \approx d_2 \approx$ half the multilamellar repeat distance in Fig. 2.

For the lipid area in the plane of the bilayer, a value of 70 $Å^2$ was considered for DOTAP (Koltover et al. 1999) and 67.5 $Å^2$ for DOTAP/DOPE (Wiethoff et al. 2003). The γ value (see also Fig. 2) is the fraction of donor molecules whose decay ($i_{D0}(t)$) is unaffected by the acceptors corresponding to the BOBO-1 molecules within free DNA.

The theoretical FRET efficiency is calculated by

$$E = 1 - \int_0^\infty i_{DA}(t)\mathrm{d}t \Big/ \int_0^\infty i_D(t)\mathrm{d}t \tag{5}$$

and can be compared with the experimental (from steady-state measurements) value, calculated using

$$E = 1 - \left(\frac{I_{DA}}{I_D}\right) \tag{6}$$

where I_{DA} and I_D are the donor fluorescence intensities in the absence and in the presence of acceptor, respectively.

In this work, the methodology to access the liposome complexation efficiency of a specific formulation (lipid/DNA in buffer) was as follows:

Step 1: Lipoplex agarose gel electrophoresis to have a first approach to the charge ratio (±) above which all the DNA is covered by the lipid (absence of free DNA).
Step 2: FRET assay with the charge ratios that were selected in step 1 (charge ratios with the absence of free DNA, and so $\gamma = 0$ was fixed), to recover the interchromophore distance (d) as the sole parameter using Eqs. 2–6.
Step 3: Considering the distance (d) fixed to the value recovered in *step 2*, the FRET assay of lipoplexes with lower charge ratios (with free DNA) enabled the recovery of the γ value. The liposome complexation efficiency (CE) was calculated by

$$\mathrm{CE} = (1 - \gamma) \times 100 \tag{7}$$

Results and discussion

The main objective of this study was to investigate the effect of certain parameters, such as charge ratio, presence of helper lipid and plasmid size, on the ability of cationic liposomes to complex DNA. Several methodologies were used simultaneously, in order to determine which is the lowest charge ratio of a given lipoplex formulation with all DNA covered by liposomes. This can help to avoid the addition of the unnecessary amount of potentially cytotoxic cationic lipid to DNA in transfection protocols.

Agarose gel electrophoresis

As a first approach to determine the efficiency and extent of liposome–DNA complex formation, lipoplexes were analysed by gel electrophoresis. At higher charge ratios, with excess of cationic liposomes, no free DNA was observed on the agarose gel (Fig. 3), which is the first sign of complete complexation of DNA within cationic liposomes.

Without DOPE, free DNA is still observed in lipoplexes with charge ratio (±) = 4 and 6 with pVAX and pVAX25, respectively (Fig. 3a, c). When DOPE is included in liposomes, all the DNA is protected at lower charge ratios, because no free DNA is observed at charge ratio (±) = 2 (Fig. 3b).

Similar results were obtained when BOBO-1 is previously added to DNA and the lipoplexes are loaded on an agarose gel (not shown). All the gels were run in duplicate, using different DNA and liposome batches, and the smear that appears in several lanes depends on the quality of the gel revelation.

Lifetime and intensity measurements of BOBO-1 in lipoplexes

To verify the binding of DNA probes to plasmid DNA in the presence of cationic liposomes, the fluorescence intensity of the dye in several lipoplex formulations were measured (Fig. 4).

For lower charge ratios (<1), BOBO-1 fluorescence is rather high and similar to that obtained without liposomes, and at higher charge ratios a decrease in fluorescence is observed (Fig. 4). Lipoplexes prepared with DOTAP and either pVAX25 or pVAX, for charge ratio = 10, have around 25% of the fluorescence intensity in the absence of liposomes. Comparing the profiles obtained for pVAX with DOTAP:DOPE (*filled triangle*) and with DOTAP (*filled diamond*), it is possible to verify that BOBO-1 fluorescence intensity, within lipoplexes with helper lipid, is approximately 20% higher than that measured with DOTAP only. On the other hand, the BOBO-1 lifetime-weighted quantum yield within lipoplexes (Table 1, $\Phi_{B(BL)}$) has a similar decreasing profile. The fact that the relative decrease of the fluorescence intensity is more pronounced than that of the lifetime can have two possible origins: partial exclusion of probe to buffer or static

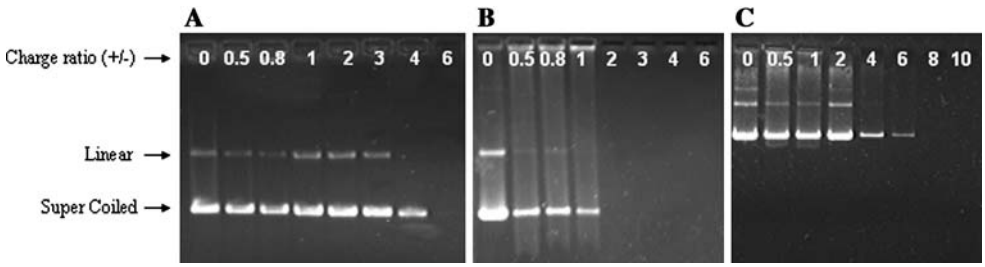

Fig. 3 Electrophoresis on agarose gel of lipoplexes. **a** DOTAP/pVAX, **b** DOTAP:DOPE/pVAX, and **c** DOTAP/pVAX25, at several charge ratios (±). [DNA] = 20 μg/mL

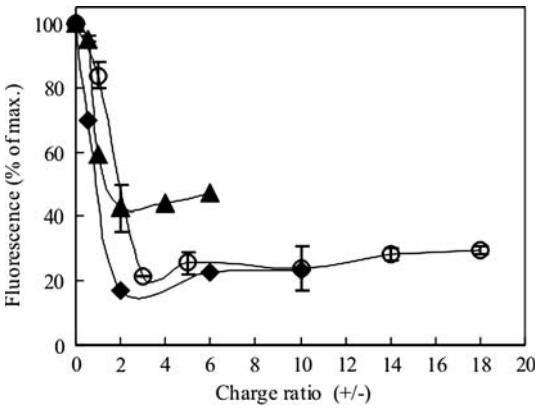

Fig. 4 BOBO-1 fluorescence in DNA within cationic liposomes. DOTAP:DOPE/pVAX (*filled triangle*); DOTAP/pVAX (*filled diamond*) DOTAP/pVAX25 (*open circle*). [DNA] = 20 μg/mL

self-quenching due to BOBO-1 aggregation upon the formation of cationic lipoplexes. In buffer, BOBO-1 fluorescence quantum yield is significantly reduced (by a factor of 500), and the fluorescence decay is extremely fast and cannot be measured by our instrument (Madeira et al. 2005) The significant drop in fluorescence intensity is partly explained by the decay data, although displacement of some of the probe into the buffer cannot be excluded. A ≈ 50% drop in lifetime-weighted quantum yield is observed for DOTAP/DNA ratios >1, indicating that BOBO-1 is intrinsically half as fluorescent in cationic lipoplexes. This would imply per se a ≈50% drop in fluorescence intensity. The 5-fold fluorescence intensity decrease seen in Fig. 4 would then denote a 2.5-fold concentration decrease of fluorescent BOBO-1 molecules, that is, ~40% of the probe would remain in the lipoplexes, whereas the remainder would be excluded to the buffer, where they are essentially not fluorescent. This 40% value must be seen as a minimal limit, as there is the possibility of static self-quenching due to BOBO-1 aggregation upon the formation of cationic lipoplexes, which would not affect the lifetime-weighted quantum yield values, but would reduce the steady-state intensities for charge ratios >1 in Fig. 4. In any case, FRET measurements using BOBO-1 as donor will not be affected, because the non-fluorescent BOBO-1 molecules will be ''silent'' for FRET purposes.

BOBO-1 fluorescence decays, shown in Table 1, are tri-exponential (with decay times 0.2–0.3, ~1 and 2–3 ns) for all DOTAP/DNA charge ratios (±),

Table 1 Decay parameters of BOBO-1 in pVAXlacZ in the presence and absence of DOTAP or DOTAP:DOPE. d/b = 0.01

Lipoplex	Charge ratio (±)	Fluorescence lifetimes (amplitudes) (ns)						$\langle\tau\rangle$ (ns)	χ^2	$\Phi_{B(BL)}$
		τ_1	(α_1)	T_2	(α_2)	τ_3	(α_3)			
DOTAP/pVAX	0	0.35	(0.29)	1.49	(0.44)	3.43	(0.27)	1.69	1.2	0.26
	0.5	0.34	(0.26)	1.25	(0.43)	2.85	(0.31)	1.50	1.1	0.23
	2	0.18	(0.46)	0.62	(0.40)	2.00	(0.14)	0.61	1.2	0.09
	4	0.22	(0.46)	0.80	(0.40)	2.48	(0.14)	0.77	1.1	0.12
	6	0.22	(0.50)	0.87	(0.37)	2.80	(0.13)	0.79	1.1	0.12
	8	0.26	(0.52)	1.10	(0.37)	3.38	(0.11)	0.91	1.0	0.14
DOTAP:DOPE/ pVAX	0.5	0.38	(0.36)	1.69	(0.48)	3.88	(0.16)	1.57	1.0	0.24
	2	0.26	(0.52)	0.95	(0.38)	2.80	(0.11)	0.79	1.1	0.12
	4	0.26	(0.49)	1.02	(0.37)	3.08	(0.14)	0.93	1.0	0.14
	6	0.30	(0.44)	1.15	(0.40)	3.21	(0.16)	1.11	1.1	0.17
DOTAP/pVAX25	0	0.26	(0.27)	1.24	(0.43)	3.22	(0.31)	1.59	1.3	0.24
	0.5	0.27	(0.26)	1.26	(0.42)	3.24	(0.32)	1.64	1.2	0.25
	1	0.25	(0.33)	1.05	(0.48)	2.77	(0.19)	1.11	1.2	0.17
	3	0.23	(0.47)	0.96	(0.39)	3.12	(0.13)	0.90	1.3	0.14
	5	0.24	(0.44)	0.99	(0.42)	3.12	(0.15)	0.97	1.3	0.15
	10	0.25	(0.41)	1.00	(0.43)	3.17	(0.16)	1.03	1.3	0.16
	14	0.27	(0.44)	1.06	(0.41)	3.30	(0.15)	1.04	1.2	0.16
	18	0.25	(0.43)	1.05	(0.42)	3.46	(0.14)	1.05	1.3	0.16

indicating probe environment heterogeneity or complex intrinsic probe photophysics. Small differences in the measured decays were observed at lower charge ratios, when compared with the lifetime components and respective amplitudes in the absence of lipid, denoting no substantial changes in DNA conformation. At higher charge ratios, changes in lifetime and amplitudes were observed, with decrease of the relative amplitude of the long-lived lifetime component and increase of the short-lived one. A similar behaviour was observed with plasmid condensed by the cationic polymer CTAB, using YOYO-1 (Clamme et al. 2000). In the case of pVAX25, for which higher lipoplex charge ratios (10–18) were studied, the similarity between their $<\tau>$ values led us to the idea that the structural arrangement of lipoplexes reaches a state, for a specific charge ratio, that becomes invariant with addition of higher quantities of lipid. The presence of DOPE in lipoplexes gives rise to an increase of $<\tau>$ for charge ratios 2–6. In all cases, a small increase of BOBO-1 $<\tau>$ when all DNA is covered by the liposome was verified.

The decrease of the dye quantum yield in the presence of liposomes cannot be explained solely assuming simple segregation of dye to buffer, because such a process would either lead to the appearance of an extremely fast decay component (arising from the segregated molecules) or leave the measured fluorescence decay unaltered (if this decay component were too fast to be detected), and would reduce the quantum yield drastically. The reductions in quantum yield and average lifetime values result primarily from a change in the probe environment upon condensation (Madeira et al. 2005). As a consequence of competition with the cationic lipid molecules for the negatively charged DNA sites, the dye molecules, while probably still bound to a significant extent, adopt a different conformation in the double helix, possibly becoming more exposed to solvent (Krishnamoorthy et al. 2002) or with a larger degree of internal rotation around the methine bridges of each chromophore [which is why these cyanine dyes are non-fluorescent in water (Carlsson et al. 1994)]. Therefore, as long as there is free DNA in solution, a significant displacement of the dye to the buffer is not probable, and probably these uncovered DNA molecules will have a higher amount of the dye. Thus, for the complete complexation of those formulations, the low fluorescence intensity results mainly from the different environment sensed by BOBO-1 molecules, although the displacement of some dye molecules into the buffer cannot be totally excluded. At higher charge ratios, with all DNA molecules being covered by the liposomes, the fluorescence intensity and the lifetime-weighted quantum yield are almost constant (Fig. 4; Table 1). Once all DNA becomes protected by the liposomes, further addition of DOTAP does not interfere with BOBO-1 fluorescence intensity or lifetime-weighted quantum yield, which is invariant with the charge ratio. (Koltover et al. 1999) suggest that in lipoplexes with excess of lipid the inter-helical distance between DNA molecules, in the same bilayer plane, is larger when compared with lipoplexes having DNA in excess. Accordingly, and relating to our case, it is probable that the same situation will occur. In this scenario the only effect of increasing DOTAP concentration would be a less dense packing of the DNA molecules, without significantly changing the microenvironment around the BOBO-1 molecules. Therefore, major changes in the latter's fluorescence are not expected.

FRET measurements

Figures 5 and 6 show a series of experiments with the FRET pair BOBO-1/BODIPY-PC, in lipoplexes with several charge ratios (±). For each charge ratio value, the FRET efficiency increases as the acceptor concentration increases, as expected. Experimental results are compared with the theoretical curves obtained with Eqs. 2–5.

Following the agarose gel electrophoresis study (see Fig. 3a, b), the data for charge ratio (±) = 6 (a) and 4 (b) (for DOTAP/pVAX and DOTAP/DOPE/pVAX lipoplexes, respectively) were analysed assuming no isolated donors (under these conditions, there is no free DNA, and all BOBO-1 donor molecules should be available for transfer), that is, γ in Eq. 2 was taken as zero. Having fixed the value of this parameter, the sole fitting variable in Eq. 2 is b, or alternatively the donor–acceptor interplanar distance $d = R_0 <\tau>^{-1/6} b^{-1/2}$. From this procedure, $d = 32$ Å is obtained in both cases (Fig. 5a, b).

When a longer plasmid (6,717 bp) is considered, the lowest charge ratio where no free DNA is observed in agarose gel (Fig. 3c) is 8. Figure 5c shows FRET experimental data for several charge ratios (5, 6, 8, 10 and 18), and their respective fitting curves. As previously, it was assumed that when all DNA is protected by the liposomes, there are no isolated donors and therefore $\gamma = 0$. The only variable is still the donor–acceptor interplanar distance (d), which is 40 Å for this lipoplex system. Curiously, at variance with what was observed in electrophoresis (for which a small amount of free DNA was still observed for (±) = 6, see Fig. 3c), lipoplexes with both charge ratio (±) = 5 or 6

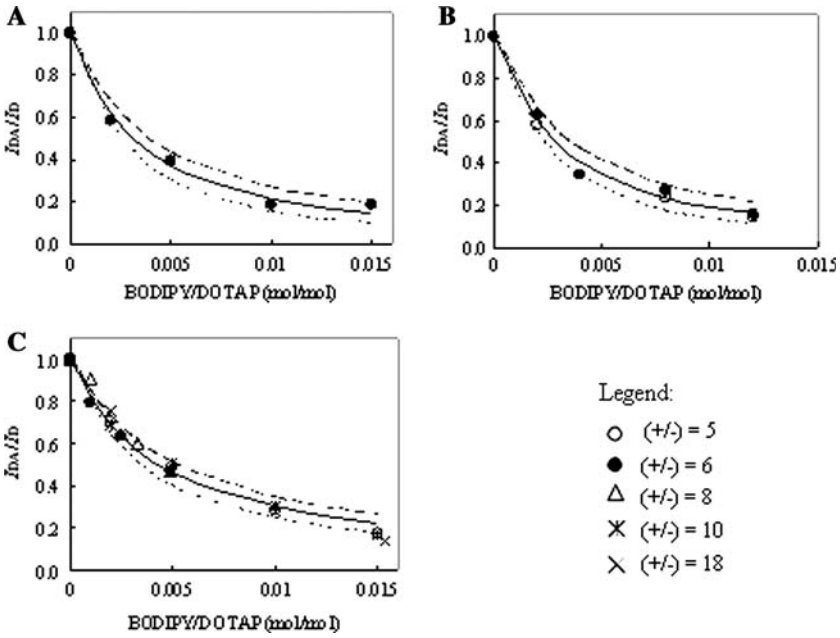

Fig. 5 FRET quenching ratios, $I_{DA}/I_D = 1 - E$, for the BOBO-1/BODIPY-PC pair in DOTAP/pVAX (**a**), DOTAP/DOPE/pVAX (**b**) and DOTAP/pVAX25 (**c**). Fitting curves using Eqs. 2–6, and parameters for (±) = 6 are shown for **a** and **c**. The assumed fitting parameters in both cases were: $\gamma = 0$ (fixed), $d = 36$ Å (*dashed line*), $d = 32$ Å (*straight line*), $d = 27$ Å (*dotted line*). Fitting curves for (±) = 5 are also shown for **c**. The assumed fitting parameters were: $\gamma = 0$ (fixed), $d = 43$ Å (*dashed line*), $d = 40$ Å (*straight line*), $d = 36$ Å (*dotted line*). [DNA] = 20 μg/mL

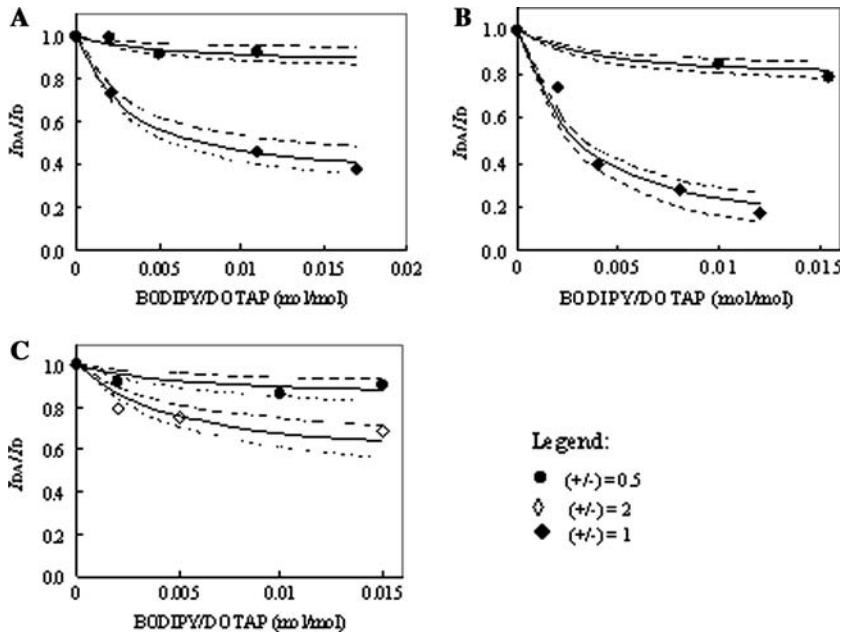

Fig. 6 FRET quenching ratios, $I_{DA}/I_D = 1 - E$, for BOBO-1/BODIPY-PC pairs in DOTAP/pVAX (**a**), DOTAP:DOPE/pVAX (**b**) and DOTAP/pVAX25 (**c**). Fitting curves using Eqs. 2–6 are shown for **a** and **c**. The assumed fitting parameters were as follows: $d = 32$ Å (fixed) in all cases, (**a**, *filled circle*) $\gamma = 0.85$ (*dashed line*), $\gamma = 0.76$ (*straight line*), $\gamma = 0.70$ (*dotted line*); (**a**, *filled diamond*) $\gamma = 0.25$ (*dashed line*), $\gamma = 0.19$ (*straight line*), $\gamma = 0.15$ (*dotted line*); (**b**, *filled circle*) $\gamma = 0.75$ (*dashed line*), $\gamma = 0.70$ (*straight line*), $\gamma = 0.65$ (*dotted line*); (**b**, *filled diamond*) $\gamma = 0.10$ (*dashed line*), $\gamma = 0.06$ (*straight line*), $\gamma = 0.00$ (*dotted line*). Fitting curves are also shown for **c**. The assumed fitting parameters were as follows: $d = 40$ Å (fixed). (*filled circle*) $\gamma = 0.85$ (*dashed line*), $\gamma = 0.75$ (*straight line*), $\gamma = 0.65$ (*dotted line*); (*filled diamond*) $\gamma = 0.50$ (*dashed line*), $\gamma = 0.40$ (*straight line*), $\gamma = 0.30$ (*dotted line*). [DNA] = 20 μg/mL

showed no isolated donors in the FRET measurements. We believe that this difference is not critical, and, given that for the DOTAP/pVAX and DOTAP/DOPE/pVAX there is in fact agreement regarding the lowest charge ratio without free DNA, both FRET and agarose gel electrophoresis are essentially reporting the same information in this study, with minor occasional discrepancies.

In this case, lipoplexes which showed free DNA on agarose gel electrophoresis (Fig. 3c) display the same FRET efficiency as that observed for higher charge ratios (10 and 18), where all DNA is protected by the liposomes. Lipoplexes containing DOPE (Fig. 5a), and with charge ratios 4 and 6 also present the same FRET profile, leading us to believe that all DNA is covered at charge ratio 4. It is important to mention that the lipoplex formulations that show higher transfection efficiencies are positively charged, have all DNA protected from endonucleases and use the lowest possible dose of cationic liposome to minimize toxicity. Thus, it is important to choose a formulation with all DNA protected by the lipoplexes, but at the same time, a very high charge ratio is unnecessary and could display cellular toxicity. In FRET studies lipoplexes are suspended in solution, similarly to when they are used in transfection studies. The decay parameters of BOBO-1 presented on Table 1 also support the claim for total complexation of DNA at charge ratios from 5 to 18 in DOTAP/pVAX25 lipoplexes, from 4 to 8 in DOTAP/pVAX lipoplexes and from 4 to 6 in lipoplexes with the same plasmid but containing also DOPE. For the referred charge ratios the lifetime components and amplitudes are very similar, revealing that BOBO-1 presents the same conformation and ''sees'' the same environment.

When lipoplexes with lower charge ratios, for which free DNA is expected to be present are analysed by this methodology, one must consider the donor–acceptor interplanar distance (d) recovered by the previous measurements, as it is known that interlamellar distance is invariant with the charge ratio (Koltover et al. 1999).

The experimental results shown in Fig. 6 illustrate the overall decrease of FRET efficiency with decreasing charge ratio, when compared to Fig. 5. When a lower lipid amount is added to DNA, for a charge ratio of 2, less FRET is observed, denoting that a small part of the DNA is not covered by the liposomes, and an even less FRET is measured for charge ratio 0.5. In this case, only a small part of BOBO-1 dye molecules, within the DNA, are in close contact with labelled liposomes.

Similar FRET profiles were obtained for lipoplexes with pure DOTAP and with DOTAP:DOPE, for charge ratios 2 and 0.5 (Fig. 6a, b). The difference is in terms of fraction of isolated donors. When DOPE is present, less isolated donors were obtained in each case, when compared with lipoplexes only with DOTAP. For charge ratio 2, $\gamma = 0.19$ with DOTAP and $\gamma = 0.06$ with DOTAP:DOPE are recovered, whereas for charge ratio 0.5, $\gamma = 0.76$ was recovered for DOTAP lipoplexes and $\gamma = 0.70$ was obtained for DOTAP:DOPE.

When a longer plasmid is used (Fig. 6c), together with pure DOTAP liposomes, a similar FRET profile was obtained. For charge ratio = 0.5, the fraction of isolated donors is very similar to that obtained with a smaller plasmid (Fig. 6a), $\gamma = 0.75$ being recovered. For charge ratio = 1, a value of 0.40 was obtained, denoting a smaller quantity of isolated donors and therefore a larger amount of DNA covered by liposomes.

Table 1 shows the BOBO-1 quantum yields obtained for all studied charge ratios, but for FRET purposes, to calculate R_0 values, only quantum yields of BOBO-1 in lipoplexes with all DNA covered by the liposomes were used. These quantum yield values were 0.12 for DOTAP/pVAX [(±) = 6], 0.14 for DOTAP:DOPE/pVAX [(±) = 4] and 0.15 for DOTAP/pVAX25 [(±) = 5)]. Similar R_0 values were obtained for all lipoplex formulations and their values are shown on Table 2. At charge ratios (±) > 2, a red-shift of 2–3 nm (maximum) was observed, in the BOBO-1 emission spectrum, because being BOBO-1 a polar dye it is sensitive to environment changes such as expected from exposure to the polar environment surrounding the lipid charged head groups.

A summary of all FRET measurements of this study is present in Table 2, with γ values converted in complexation efficiency (CE). Results concerning pUC19 previously published (Madeira et al. 2003) are also shown on this table for an easier comparison with other lipoplex formulations. The lipoplex system from which it is possible to verify complete DNA complexation for a lower charge ratio is the one that includes DOPE in its formulation. The main role of DOPE is to facilitate membrane fusion. Because of its ability to increase transfection rates in certain conditions, its effect on DNA complexation has been frequently studied (Eastman et al. 1997). From the obtained results, with the used methodologies, it was verified that the presence of DOPE allows better complexation of DNA. Despite the absence of free DNA detected on the agarose gel (Fig. 3b) for (±) = 2, the existence of a small quantity of uncovered DNA (6%) was verified by FRET analysis. Interestingly, using binding isoterms, an estimation of 98% was made for coverage of a 4.8 kb plasmid by DOTAP:DOPE liposomes in similar buffer conditions with the same charge ratio [(±) = 2] (Hirsh-Lerner and Barenholz 1999). For charge ratio 0.5, DOPE also plays the same role, although to less effect: 5% more DNA is being covered by the liposomes. In fact, an enhanced surrounding of plasmid DNA by lipids when DOPE is present was previously

Table 2 Complexation efficiencies (Eq. 7) for the systems in study

Lipoplex type/formulation	pDNA size (bp)	Multilamellar repeat distance		R_0 (Å)	Complexation efficiency	
		(±)	d (Å)		(±)	CE (%)
DOTAP/pUC19 [8]	2,694	4	27	41.0	4	100
					2	80
					0.5	50
DOTAP/pVAX	6,050	6	32	41.0	6	100
					2	81
					0.5	24
DOTAP:DOPE/pVAX					6	100
	6,050	4–6	32	42.0	4	100
					2	94
					0.5	30
					6	100
DOTAP/pVAX25	6,717	5–18	40	42.0	5	100
					1	60
					0.5	25

confirmed (Zuidam and Barenholz 1998). In agreement, CD measurements with DOTAP/DOPE lipoplexes denoted the appearance of a tertiary structure (ψ^-) of DNA, which is an indication of relatively proximity of parallel helices (Zuidam et al. 1999a). Gouy-Chapman calculations made by these authors verified that the presence of helper lipid in 1:1 molar ratio with the cationic lipid has a large effect on the surface positive charge density, matching better the negative charge distribution in DNA (in B-conformation) than DOTAP alone (Zuidam and Barenholz 1998).

According to our FRET results, and considering charge ratio (±) = 2, the presence of DOPE has increased in about 15% the quantity of covered DNA (Table 2). On the other hand, the presence of DOPE increases the fluorescence intensity values by 20%, when compared with the formulation without the helper lipid (Fig. 4). BOBO-1 lifetime-weighted quantum yields are also slightly higher, especially for (±) > 2. It is unlikely that a smaller quantity of the dye is displaced, when DOPE is present, at higher charge ratios, as claimed by others when using different DNA intercalators (EtBr and DAPI, a minor groove binding dye) (Wiethoff et al. 2003). These authors suggested that the half-charge density sensed by the DNA, when DOTAP:DOPE (1:1) is used, may be responsible for a smaller competition, with the dye, for binding to the negatively charged DNA. When compared with these dyes, BOBO-1 has a significantly higher affinity to the DNA.

DOTAP:DOPE lipoplexes' structures adopt a columnar inverted hexagonal phase H_{II}^c when DOPE molar fraction (χ) exceeds 0.75, whereas a pure lamellar phase (L_α^c) is present when $\chi_{DOPE} < 0.41$. Between these values, a coexistence of both structures is described (Koltover et al. 1998). In our studies $\chi_{DOPE} = 0.50$ (± 0.02) was used. Even so, the application on these lipoplexes of the multilamellar biophysical models led to reasonable results. In other words, a good fit to experimental results of the DOTAP:DOPE lipoplexes [$\chi_{DOPE} = 0.50$ (±0.02)] was obtained when equations derived from a multilamellar distribution of DNA between lipid bilayers were used. This is not too surprising, because for $\chi_{DOPE} = 0.50$, the expected fraction of H_{II}^c phase is according to the lever rule (Atkins 2002) (0.50–0.41)/(0.75–0.41) ≈ 26%, and therefore the system is still mainly in the lamellar phase. Model fitting (Eq. 2) to experimental values obtained for lipoplexes with (= 4 led to an inter-chromophore distance of 32 Å. For this charge ratio, the DNA is covered by the liposomes, as revealed from the agarose gel and fluorescence measurements. On the other hand, upon DNA complexation with liposomes, a dehydration effect on DNA was observed with DOTAP:DOPE rather than with DOTAP (Choosakoonkriang et al. 2001; Hirsh-Lerner and Barenholz 1999), which according to our results, may not affect greatly the inter-chromophore or multilamellar distances (but may contribute to the enhanced BOBO-1 fluorescence in the presence of DOPE). A major dehydrating effect is verified, on the DNA bases, upon addition of liposomes containing a higher DOPE molar ratio (Choosakoonkriang et al. 2001). Using a similar FRET assay, where a distance of closest approach (L) of DNA to the lipid bilayer was recovered, yet using a different mathematical approach, Wiethoff et al. (2002) also reported that DOTAP:DOPE lipoplexes show similar trend in L compared with DOTAP lipoplexes.

The donor–acceptor distance varies with the plasmid size, because when longer plasmids are used (pVAX-

lacZ and pVAXlacZp24, 6,050 or 6,717 bp respectively), larger (32 and 40 Å, respectively) distances are obtained, versus 27 Å with a smaller plasmid (pUC19, 2,694 bp) (Madeira et al. 2003). In fact, the two longer plasmids showed similar complexation profiles for charge ratio 0.5 (~25%), whereas 50% of DNA complexation was obtained with the smaller plasmid. Despite different charge ratios having been studied, above (±) = 0.5 similar values were obtained (60% for DOTAP/pVAX25 with (±) = 1 and 80% for DOTAP/pVAX and DOTAP/pUC19 with (±) = 2). However, the reason for the significant difference (8 Å) between the pVAXlacZ and pVAXlacZp24 repeat distances is not clear and cannot be attributed solely to plasmid size (the latter is only ~10% larger).

Conclusions

In this work, using FRET with different plasmids and liposome formulations, we showed that, despite the complexity of these systems not being totally described by our model, not only the utility of this technique on lipoplex study was confirmed, but also further insight about lipoplex structure in low ionic strength solution was obtained. It can be concluded that (1) once all DNA is covered by the liposomes, additional lipid molecules do not affect the lipoplex multilamellar repeat distance and, presumably, lipoplex structure becomes invariant; (2) the presence of helper lipid DOPE reduces the amount of cationic lipid required for DNA protection but does not affect the lipoplex multilamelar repeat distance; (3) there is some indication that this distance varies with the plasmid size when supercoiled plasmid is used, being larger when longer plasmids are used.

Acknowledgments C. M. acknowledges financial support from FCT, PRAXIS XXI (BD/21476/1999), Portugal. L. M. S. L., A. F. and M. P. acknowledge financial support from POCTI projects (FCT).

References

Atkins PW (2002) Physical chemistry, 7th edn. Oxford University Press, Oxford

Caracciolo G, Caminiti R, Pozzi D, Friello M, Boffi F, Castellano AC (2002) Self-assembly of cationic liposomes-DNA complexes: a structural and thermodinamic study by EDXD. Chem Phys Lett 351:222–228

Carlsson C, Larsson A, Jonsson M, Albinsson B, Norden B (1994) Optical and photophysical properties of the oxazole yellow DNA probes Yo and Yoyo. J Phys Chem 98:10313–10321

Choosakoonkriang S, Wiethoff CM, Anchordoquy TJ, Koe GS, Smith JG, Middaugh CR (2001) Infrared spectroscopic characterization of the interaction of cationic lipids with plasmid DNA. J Biol Chem 276:8037–8043

Clamme JP, Bernacchi S, Vuilleumier C, Duportail G, Mély Y (2000) Gene transfer by cationic surfactants is essentially limited by the trapping of the surfactant/DNA complexes onto the cell membrane: a fluorescence investigation. Biochim Biophys Acta 1467:347–361

Eastman SJ, Sigel C, Tousignant J, Smith AE, Cheng SH, Scheule RK (1997) Biophysical characterization of cationic lipid:DNA complexes. Biochim Biophys Acta 1325:41–62

Farhood H, Serbina N, Huang L (1995) The role of dioleoyl phosphatidylethanolamine in cationic liposome mediated gene transfer. Biochim Biophys Acta 1235:289–295

Ferrari ME, Rusalov D, Enas J, Wheeler CJ (2001) Trends in lipoplexes physical properties dependent on cationic lipid structure, vehicle and complexation procedure do not correlate with biological activity. Nucleic Acids Res 29:1539–1548

Gershon H, Ghirlando R, Guttman SB, Minsky A (1993) Mode of formation and structural features of DNA-cationic liposome complexes used for transfection. Biochemistry 32:7143–7151

Hirsh-Lerner D, Barenholz Y (1999) Hydration of lipoplexes commonly used in gene delivery: follow-up by laurdan fluorescence changes and quantification by differential scanning calometry. Biochim Biophys Acta 1461:47–57

Hong K, Zheng W, Baker A, Papahadjopoulos D (1997) Stabilization of cationic liposome-plasmid DNA complexes by polyamines and poly(ethylene glycol)-phospholipid conjugates for efficient in vivo gene delivery. FEBS Lett 400: 233–237

Huang L, Hung M-C, Wagner E (1999) Non viral vectors for gene therapy. Academic, San Diego

Itaka K, Harada A, Nakamura K, Kawaguchi H, Kataoka K (2002) Evaluation by fluorescence resonance energy transfer of nonviral gene delivery vectors under physiological conditions. Biomacromolecules 3:841–845

Koltover I, Salditt T, Radler JO, Safinya CR (1998) An inverted hexagonal phase of cationic liposome-DNA complexes related to DNA release and delivery. Science 281:78–81

Koltover I, Salditt T, Safinya CR (1999) Phase diagram, stability, and overcharging of lamellar cationic lipid-DNA self-assembled complexes. Biophys J 77:915–924

Kreiss P, Cameron B, Rangara R, Mailhe P, Aguerre-Charriol O, Airiau M, Scherman D, Crouzet J, Pitard B (1999) Plasmid DNA size does not affect the physicochemical properties of lipoplexes but modulates gene transfer efficiency. Nucleic Acids Res 27:7392–3798

Krishnamoorthy G, Duportail G, Mély Y (2002) Structure and dynamics of condensed DNA probed by 1,1′-(4,4,8,8-tetramethyl-4,8-diazaundecamethylene)bis[4-[[3-methylbenz-1,3-oxazol-2-yl]methylidine]-1,4-dihydroquinolinium] tetraiodide fluorescence. Biochemistry 41:15277–15287

Lasic DD, Strey H, Stuart MCA, Podgornik R, Frederik PM (1997) The structure of DNA-liposome complexes. J Am Chem Soc 119:832–833

Lee RJ, Huang L (1996) Folate-targeted, anionic liposome-entrapped polylysine-condensed DNA for tumor cell-specific gene transfer. J Biol Chem 271:8481–8487

Lleres D, Dauty E, Behr J-P, Mély Y, Duportail G (2001) DNA condensation by an oxidizable cationic detergent. Interactions with lipid vesicles. Chem Phys Lipids 111:59–71

Lleres D, Clamme JP, Dauty E, Blessing T, Krishnamoorthy G, Duportail G, Mely Y (2002) Investigation of the stability of dimeric cationic surfactant/DNA complexes and their

interaction with model membrane systems. Langmuir 18:10340–10347
Loura LMS, Fedorov A, Prieto M (2001) Fluid–fluid membrane microheterogeneity: a fluorescence resonance energy transfer study. Biophys J 80:776–788
Madeira C, Loura LM, Aires-Barros MR, Fedorov A, Prieto M (2003) Characterization of DNA/lipid complexes by fluorescence resonance energy transfer. Biophys J 85:3106–3119
Madeira C, Fedorov A, Aires-Barros MR, Prieto M, Loura LMS (2005) Photophysical behaviour of a dimeric cyanine dye (BOBO-1) within cationic liposomes. Photochem Photobiol 81:1450–1459
Marquardt DW (1963) An algorithm for least-squares estimation of non-linear parameters. J Soc Ind Appl Math 11:431–441
Oberle V, Bakowsky U, Zuhorn IS, Hoekstra D (2000) Lipoplex formation under equilibrium conditions reveals a three-step mechanism. Biophys J 79:1447–1454
Perrie Y, Gregoriadis G (2000) Liposome-entrapped plasmid DNA: characterization studies. Biochim Biophys Acta 1475:125–132
Rädler JO, Koltover I, Salditt T, Safinya CR (1997) Structure of DNA-cationic liposome complexes: DNA intercalation in multilamellar membranes in distinct interhelical packing regimes. Science 275:810–814
Radler JO, Koltover I, Jamieson A, Salditt T, Safinya CR (1998) Structure and interfacial aspects of self-assembled cationic lipid-DNA gene carrier complexes. Langmuir 14:4272–4283
Ross PC, Hui SW (1999) Lipoplex size is a major determinant of in vitro lipofection efficiency. Gene Ther 6:651–659
Simões S, Slepushkin V, Pires P, Gaspar R, Lima MCPd, Duzgunes N (2000) Human serum albumin enhances DNA transfection by lipoplexes and confers resistance to inhibition by serum. Biochim Biophys Acta 1463:459–469
Smisterová J, Wagenaar A, Stuart MCA, Polushkin E, Brinke G, Hulst R, Engberts JBFN, Hoekstra D (2001) Molecular shape of the cationic lipid controls the structure of cationic lipid/dioleylphosphatidylethanolamine-DNA complexes and the efficiency of gene delivery. J Biol Chem 276:47615–47622
Templeton NS, Lasic DD, Frederik PM, Strey HH, Roberts DD, Pavlakis GN (1997) Improved DNA:liposome complexes for increased systemic delivery and gene expression. Nat Biotechnol 15:647–652
Thierry AR, Rabinovich P, Peng B, Mahan LC, Bryant JL, Gallo RC (1997) Characterization of liposome-mediated gene delivery: expression, stability and pharmacokinetics of plasmid DNA. Gene Ther 4:226–237
Wiethoff CM, Gill ML, Koe GS, Koe JG, Middaugh CR (2002) The structural organization of cationic lipid-DNA complexes. J Biol Chem 277:44980–44987
Wiethoff CM, Gill ML, Koe GS, Koe JG, Middaugh CR (2003) A fluorescence study of the structure and accessibility of plasmid DNA condensed with cationic gene delivery vehicles. J Pharm Sci 92:1272–1285
Wong M, Kong S, Dragowska WH, Bally MB (2001) Oxazole yellow homodimer YOYO-1-labeled DNA: a fluorescent complex that can be used to assess structural changes in DNA following formation and cellular delivery of cationic lipid DNA complexes. Biochim Biophys Acta 1527:61–72
Zhang Y, Garzon-Rodriguez W, Manning MC, Anchordoquy TJ (2003) The use of fluorescence resonance energy transfer to monitor dynamic changes of lipid-DNA interactions during lipoplex formation. Biochim Biophys Acta 1614:182–192
Zhou X, Huang L (1994) DNA transfection mediated by cationic liposomes containing lipopolylysine: characterization and mechanism of action. Biochim Biophys Acta 1189:195–203
Zuidam NJ, Barenholz Y (1998) Electrostatic and structural properties of complexes involving plasmid DNA and cationic lipids commonly used for gene delivery. Biochim Biophys Acta 1368:115–128
Zuidam NJ, Barenholz Y, Minsky A (1999a) Chiral DNA packaging in DNA-cationic liposome assemblies. FEBS Lett 457:419–422
Zuidam NJ, Hirsh-Lerner D, Margulies S, Barenholz Y (1999b) Lamellarity of cationic liposomes and mode of preparation of lipoplexes affect transfection efficiency. Biochim Biophys Acta 1419:207–220